

## Single-channel recordings of two types of calcium channels in rat pancreatic $\beta$ -cells

Salvador Sala and Donald R. Matteson

University of Maryland School of Medicine, Department of Biophysics, Baltimore, Maryland 21201 USA

**ABSTRACT** Using the cell-attached configuration of the patch clamp technique, we have identified two different types of Ca channels in rat pancreatic  $\beta$ -cell membranes. The two channels differ in single channel conductance, voltage dependence, and inactivation properties. The single-channel conductance, measured with 100 mM  $Ba^{2+}$  in the pipette, was 21.8 pS for the large channel and 6.4 pS for the small channel. The large-conductance channel is similar to the fast deactivating or L-type Ca channel described in other preparations. It is voltage dependent, has a threshold for activation around  $-30$  mV, and can be activated from a holding potential of  $-40$  mV. On the other hand, the small-conductance Ca channel is similar to the SD or T type Ca channel; it has a lower activation threshold, around  $-50$  mV, and it can be inactivated by holding the membrane potential at  $-40$  mV.

### INTRODUCTION

Pancreatic  $\beta$ -cells secrete insulin in response to an increase in the extracellular glucose concentration. These cells exhibit glucose-induced electrical activity consisting of oscillations in the membrane potential between a hyperpolarized phase and an active phase made up of a burst of spikes superimposed on a plateau depolarization (Dean and Matthews, 1968, 1970). Several types of ionic channels are thought to be involved in the generation of electrical activity in  $\beta$ -cells. Voltage-dependent Ca channels are particularly important because of their role in controlling the intracellular free  $Ca^{2+}$  concentration and, thereby, the secretion of insulin.

Experiments done using the whole cell configuration of the patch clamp technique have shown that Ca tail currents in rat pancreatic  $\beta$ -cells are made up of two distinct components: a fast deactivating (FD) and slow deactivating (SD) component (Hiriart and Matteson, 1988), similar to those described in other preparations (Armstrong and Matteson, 1985; Cota, 1986). Analysis of these tail currents indicated that  $\beta$ -cells have two types of Ca channels which differ in voltage dependence, inactivation, selectivity, and sensitivity to washout. These experiments suggested that the Ca channel types underlying the FD and SD components have properties similar to L- and T-type Ca channels, respectively, described by others (Bean, 1989). However, this result has been controversial, mainly because single-channel recordings from mouse  $\beta$ -cells have revealed only a single population of L-type Ca channels (Rorsman et al., 1988). Recently, recordings of large- and small-conductance Ca channels in rat  $\beta$ -cells were reported, although the properties of the channels were not described in detail (Ashcroft et al.,

1990). In addition, kinetic analysis of whole-cell Ca currents in rat  $\beta$ -cells suggested the presence of two populations of channels (Hidalgo et al., 1989). Because of its low activation threshold, the T-type calcium channel could play an important role in the generation of plateau depolarizations.

In this paper, an analysis of single-channel recordings from rat pancreatic  $\beta$ -cells provides further evidence for two different types of Ca channels with properties corresponding to FD and SD tail currents. Hereafter, we will refer to the larger conductance channel as L, and the smaller conductance channel as T. A preliminary report of some of our results has been presented elsewhere (Sala and Matteson, 1990).

### METHODS

#### Cell isolation and culture

The rat pancreas was excised and rinsed with ice cold Hank's Balanced Salt Solution (HBSS). The pancreas was then minced and digested with type IV collagenase. After digestion the tissue was washed with HBSS, and the islets were hand picked with a Lang-Levi pipette at least three times to separate them from the acinar tissue. The islets were washed with a Spinner salt solution containing EGTA, incubated for 10 min at  $37^{\circ}C$  and dispersed mechanically with a Pasteur pipette. The cells were washed three times in RPMI and plated onto coverslips in RPMI containing 10% fetal bovine serum, 2 mM glutamine, 100 U/ml penicillin, and 100  $\mu$ g/ml streptomycin. The cells were maintained in culture, at  $37^{\circ}C$  in a 5%  $CO_2$  incubator, for up to 1 wk.

#### Patch-clamp recording and analysis

We have used the cell-attached configuration of the patch-clamp technique (Hamill et al., 1981) to record single-channel currents. Patch

pipettes were coated with sylgard and fire polished. The output of an Axopatch-1B amplifier was filtered at 2 kHz with an eight-pole Bessel filter, and sampled with a 14-bit A/D converter at a sampling rate of 20 kHz, using a 386 computer (Compaq Computer Corp., Houston, TX). Voltage pulses were applied at 1 Hz using a 14-bit D/A converter controlled by the computer. We designed and built the hardware interface used to control both the A/D and the D/A converters, and wrote the software necessary to run the interface in the C programming language. Linear capacitive and leak currents were removed by subtracting an average of several records without channels openings. All experiments were done at room temperature, 22–24°C.

Amplitude histograms were fit to a sum of gaussian distributions of the form  $y(x) = \sum A_n \exp \{-[(x - B_n)/C_n]^2\}$ , where  $x$  is the current amplitude, and for the  $n$ th gaussian  $A_n$  is the maximum number of events,  $B_n$  is the mean amplitude, and  $C_n$  is the width. Fits were obtained by minimizing chi-square using the Levenberg-Marquardt method.

The amplitude histograms that we analyze here have a maximum of three peaks: one corresponding to no open channels, one to openings of a single T channel, and one to openings of a single L channel. The area under one of the open-channel peaks is a measure of the total open time of that channel. Therefore,  $Np_0$  (i.e., the number of channels in the patch times the open probability) can be estimated from the relative area of the corresponding gaussian distribution:  $(A_n C_n)/(\sum A_n C_n)$ . This method would underestimate  $Np_0$  for T channels at positive voltages where openings of T and L channels often overlap. The simultaneous opening of one T- and one L-type channel produces a large current (i.e., events in the peak corresponding to L channel openings) which would not contribute to the estimate of  $Np_0$  for T channels.

## Solutions

The composition of the bath solution was (in millimolar): 135 KCl, 1 MgCl<sub>2</sub>, 10 Hepes, 10 EGTA, pH 7.35 with KOH. This solution was used to zero the resting potential of the cell so that the membrane potential of the cell-attached patch could be controlled at a known level (c.f. Fox et al., 1987). In some experiments, 0.5 μM BAY K 8644 was added to the external solution to increase the open time of the L-type Ca channel. We have used 200 nM TTX to block Na channels, because we previously found that this concentration completely blocked the Na channels in rat β-cells (c.f. Hiriart and Matteson, 1988). The pipette solution used to measure the single-channel conductance was (in millimolar): 100 BaCl<sub>2</sub>, 10 TEACl, 10 Hepes, 200 nM TTX, pH 7.2 with NaOH. In the rest of the experiments the BaCl<sub>2</sub> concentration was reduced to 20 mM and the TEACl concentration was increased to maintain constant osmolarity.

## RESULTS

### Two types of calcium channels with different conductances

Fig. 1 shows single-channel recordings taken from a rat pancreatic β-cell in the cell-attached configuration. There are two distinct current levels corresponding to channel openings, indicating the existence of two populations of channels. In control experiments, no channel openings were seen when we eliminated the divalent cations from the pipette solution suggesting that the inward currents are carried by Ba<sup>2+</sup> ions.

The single-channel conductance of the two types of Ca

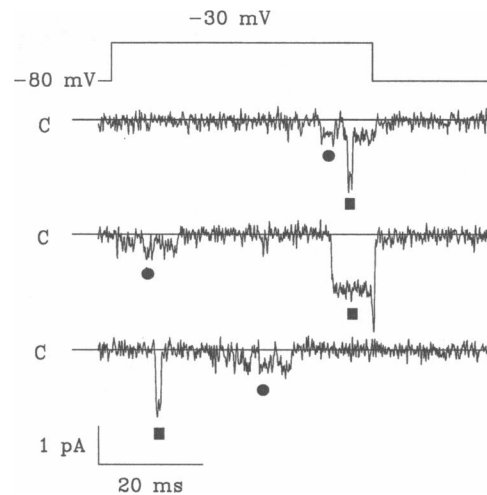


FIGURE 1 Single-channel recordings, showing two different current levels in the same patch. *C* by each trace marks the zero current level, which corresponds to all channels closed. The large (solid squares) and small (solid circles) inward current levels are ~1.5 pA and 0.5 pA, respectively. The patch potential was held at -80 mV and stepped to -30 mV for 50 ms.

channels was measured as shown in Fig. 2. Current amplitudes were measured during 50-ms pulses from a holding potential of -80 mV. Fig. 2 *A* illustrates several records taken from patches containing only one type of Ca channel, and Fig. 2 *B* shows the single-channel current-voltage relationship. The conductance estimated by the slope of a straight line fit was different for the two channels: 21.8 pS for the large-conductance L channel and 6.4 pS for the small-conductance T channel. The fact that the extrapolated reversal potential of these currents is at a positive voltage rules out the possibility that Cl channels or unblocked Na channels carry the current.

### Differences in voltage dependence

The two types of Ca channels differ in their activation threshold as shown in Fig. 3. Fig. 3 *A* shows records from a patch containing both types of Ca channels. When the membrane potential is stepped from -80 to either -50 or -40 mV, openings of only the T type Ca channels can be seen. However, when the depolarization is increased to potentials more positive than -40 mV, openings of the L-type Ca channel appear.

To further characterize the voltage dependence, we have calculated  $Np_0$  for the two channel types at various membrane potentials. Fig. 3, *B* and *C*, shows amplitude histograms measured at -40 and -20 mV, respectively. The highest peak in each histogram, centered around 0 pA, corresponds to no open channels. The other peaks

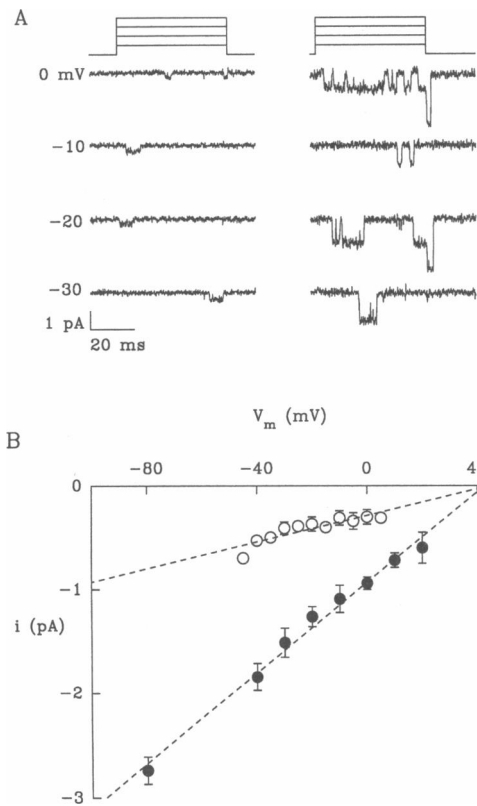


**FIGURE 2** (A) Recordings from two patches with different types of Ca channels. The pulse protocol used in these experiments is shown at the top. In each case, the patch potential was held at  $-80$  mV and changed for 50 ms to the levels indicated to the left of the current traces. The current records on the left side of the figure are from a patch that had only one small-conductance Ca channel. The records on the right part of the figure are from a patch that contained one large-conductance Ca channel. The second level of current seen in the records obtained at 0 mV and  $-20$  mV is due to a change in the driving force when the membrane potential goes back to  $-80$  mV. (B) Current-voltage relationship for the two types of Ca channels. The Ba concentration in the pipette was 100 mM. The data are plotted as mean  $\pm$  SD from 27 (solid circles) or 10 (open circles) patches. The slopes of the fitted straight lines are  $6.4 \pm 0.5$  pS and  $21.8 \pm 1.4$  pS.

represent openings of T-type channels (solid circle) or L-type channels (solid square). The relative area under these peaks is a measure of  $Np_0$ , as described in Methods. The histograms show that at  $-40$  mV there is significant T, but no L, channel activity, and at  $-20$  mV there is an increase in the activity of both channel types. Fig. 3 D is a plot of  $Np_0$  versus the membrane potential. It is clear that the frequency of openings of both Ca channels increases with membrane depolarization, and that the T-type Ca channel has a lower activation threshold than the L-type Ca channel. Similar results were obtained in six other patches.

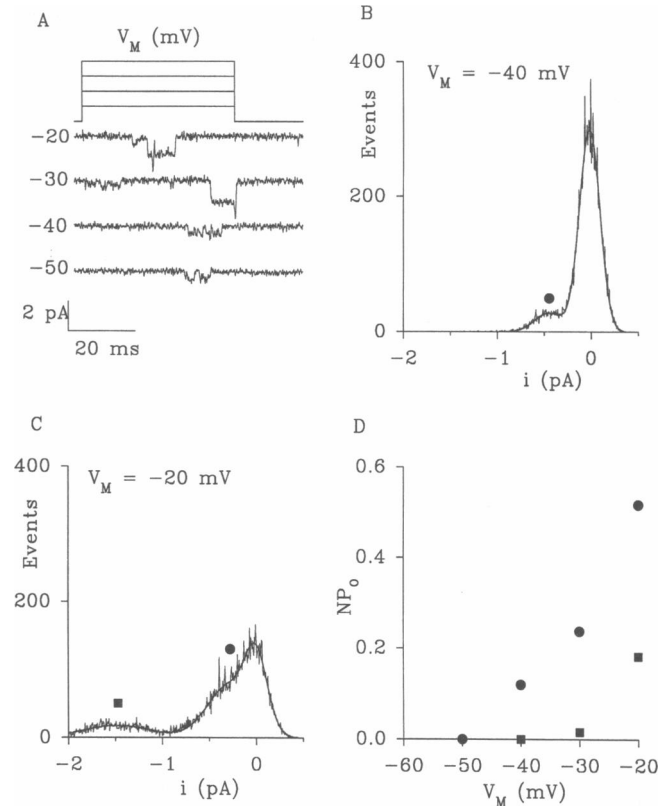


**FIGURE 3** Voltage dependence of the two types of Ca channels. (A) In these records the patch potential was held at  $-80$  mV and stepped for 50 ms to the values shown at the left of each trace. Only the small-conductance Ca channel can be seen at membrane potentials negative to  $-40$  mV. For more depolarized membrane potentials, openings of both channels can be seen. (B) Amplitude histogram made from 30 sweeps of 50 ms duration at  $-40$  mV. The data were fitted to a sum of two Gaussians, and the fit can be seen in the plot as a smooth line. The circle indicates the position of the mean current corresponding to T channel openings. (C) Amplitude histogram made from 30 sweeps at  $-20$  mV. A third peak appears, corresponding to the openings of L-type Ca channels. The circle and the square are centered on the mean currents for the T- and L-type channels, respectively. (D)  $Np_0$ , calculated as described in the Methods, is plotted vs. voltage for T (solid circles) and L (solid squares) type Ca channels.

### Differences in inactivation

Another property that distinguishes the two types of Ca channels is their inactivation at different holding potentials. The records in Fig. 4 are taken from a patch containing both types of Ca channels. Pulses to  $-20$  mV from a holding potential of  $-80$  mV activate both channel types (Fig. 4 A). However, when the membrane potential is held at  $-40$  mV in the same patch, pulses to  $-20$  mV activate only the L-type Ca channel (Fig. 4 B). A further analysis of the difference in inactivation is shown in Fig. 4, C and D. When the holding potential is  $-80$  mV, the

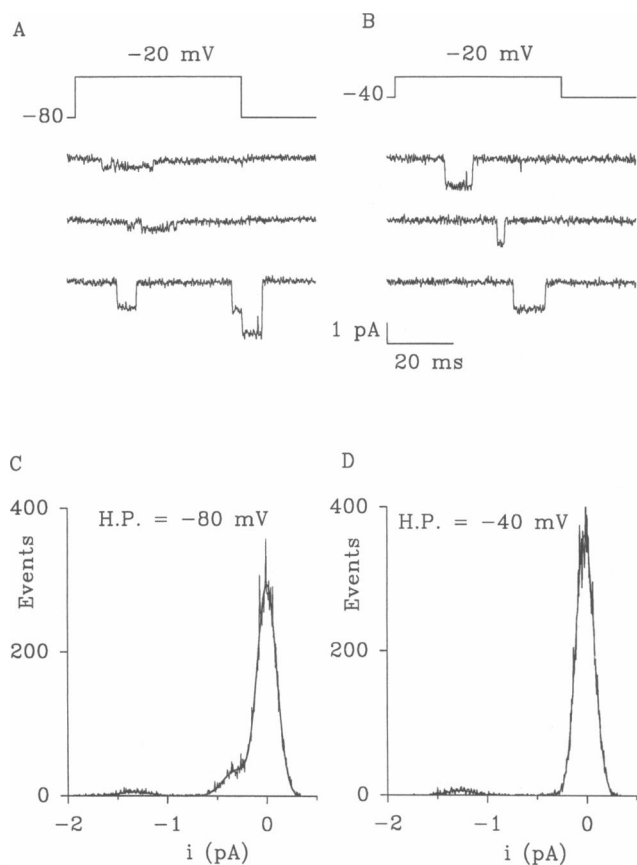


**FIGURE 4** Differences in inactivation properties of the two types of Ca channels. (A) Single-channel recordings during 50-ms pulses to  $-20$  mV from a holding potential of  $-80$  mV. Openings of both types of Ca channels are seen. (B) When the membrane potential is held at  $-40$  mV, pulses to  $-20$  mV only activate the L-type channel. Records in A and B are from the same patch. (C) Amplitude histogram made from 30 sweeps recorded during 50-ms steps to  $-20$  mV from a holding potential of  $-80$  mV. The openings of the T-type calcium channel are clearly reflected in the amplitude histogram as a peak centered around  $-0.31$  pA. The openings of the L channel are also gaussian distributed with a mean of  $-1.33$  pA. (D) Amplitude histogram obtained from the same patch as in C with the holding potential at  $-40$  mV. The T channel is inactivated and only the peak corresponding to the L channel is seen.

amplitude histogram shows peaks corresponding to L- and T-type channels (Fig. 4 C). However, when the holding potential is  $-40$  mV only the L channel peak is present. Similar results were obtained in five other patches.

## DISCUSSION

These experiments provide evidence that rat pancreatic  $\beta$ -cells have at least two different types of Ca channels. These channels differ in their conductance, voltage depen-

dence, and inactivation. The 22-pS Ca channel is similar to the L-type channel described in other preparations. It is activated at relatively positive voltages, can be activated from a holding potential of  $-40$  mV, and is sensitive to the dihydropyridine BAY K 8644 (Sala and Matteson, 1990). On the other hand, the small-conductance Ca channel is similar to the T-type channel; it has a lower voltage threshold for activation than the L channel and it is inactivated by holding the membrane potential at  $-40$  mV.

Two different types of Ca channels have been found in several vertebrate cell types (see Bean, 1989 for a review) but the presence of two types of Ca channels in pancreatic  $\beta$ -cells has remained controversial. Whole-cell (Rorsman and Trube, 1986) and single-channel experiments (Rorsman et al., 1988) done in mouse  $\beta$ -cells have revealed the presence of only one type of Ca channel, identified as the L-type channel. On the other hand, experiments done in rat  $\beta$ -cells showed that Ca tail currents were made up of two components which differed in selectivity, voltage dependence, and inactivation properties, indicating the presence of two different populations of Ca channels (Hiriart and Matteson, 1988). Other studies of whole-cell Ca currents suggesting the presence of two kinetically distinct components (Hidalgo et al., 1989) or showing a hump in the Ca I-V curve (Satin and Cook, 1988) provide additional evidence for two types of Ca channels in rat  $\beta$ -cells. A preliminary report of single-channel recordings has apparently confirmed the existence of two types of Ca channels in rat  $\beta$ -cells (Ashcroft et al., 1990). It appears that these channels are similar to those described here, although no data are shown on the voltage dependence or inactivation properties of these channels.

The two types of Ca channels could have different functions in  $\beta$ -cells. It is generally accepted that L-type channels are involved in spike generation. This is consistent with their apparent lack of inactivation at membrane potentials near the plateau level. T-type Ca channels could also play an important role in shaping the complex pattern of electrical activity characteristic of  $\beta$ -cells. For example, they could be involved in the generation of the plateau depolarization. If so, it is unlikely that they participate in the maintenance of the plateau because of their inactivation properties.

This work was supported by National Institute of Diabetes, Digestive and Kidney Diseases grant DK33212 to D. R. Matteson and by a fellowship to S. Sala from the Generalitat Valenciana.

Received for publication 9 March 1990 and in final form 2 May 1990.

---

## REFERENCES

- Armstrong, C. M., and D. R. Matteson. 1985. Two distinct populations of calcium channels in a clonal line of pituitary cells. *Science (Wash. DC)*. 227:65–67.
- Ashcroft, F. M., R. P. Kelly, and P. A. Smith. 1990. Two types of Ca channel in rat pancreatic B-cells. *Pfluegers Arch. Eur. J. Physiol.* 415:504–506.
- Bean, B. P. 1989. Classes of calcium channels in vertebrate cells. *Annu. Rev. Physiol.* 51:367–384.
- Cota, G. 1986. Calcium channel currents in pars intermedia cells of the rat pituitary gland. Kinetic properties and washout during intracellular dialysis. *J. Gen. Physiol.* 88:83–105.
- Dean, P. M., and E. K. Matthews. 1968. Electrical activity in pancreatic islet cells. *Nature (Lond.)*. 219:389–390.
- Dean, P. M., and E. K. Matthews. 1970. Glucose-induced electrical activity in pancreatic islet cells. *J. Physiol. (Lond.)*. 246:459–478.
- Fox, A. P., M. C. Nowycky, and R. W. Tsien. 1987. Single-channel recordings of three types of calcium channels in chick sensory neurones. *J. Physiol. (Lond.)*. 394:173–200.
- Hamill, O. P., A. Marty, E. Neher, B. Sakmann, and F. Sigworth. 1981. Improved patch-clamp techniques for high-resolution current recording from cells and cell-free membrane patches. *Pfluegers Arch. Eur. J. Physiol.* 391:85–100.
- Hidalgo, J., M. Y. Li, I. Atwater, and E. Rojas. 1989. Calcium currents in rat pancreatic B cells in culture. *Biophys. J.* 55:436a. (Abstr.)
- Hiriart, M., and D. R. Matteson. 1988. Na and two types of Ca channels in rat pancreatic B cells identified with the reverse hemolytic plaque assay. *J. Gen. Physiol.* 91:617–639.
- Rorsman, P., and G. Trube. 1986. Calcium and delayed potassium currents in mouse pancreatic B-cells under voltage-clamp conditions. *J. Physiol. (Lond.)*. 374:531–550.
- Rorsman, P., F. M. Ashcroft, and G. Trube. 1988. Single Ca channel currents in mouse pancreatic B-cells. *Pfluegers Arch. Eur. J. Physiol.* 412:597–603.
- Sala, S., and D. R. Matteson. 1990. Single channel recordings of calcium channels in pancreatic B cells. *Biophys. J.* 57:525a. (Abstr.)
- Satin, L. S., and D. L. Cook. 1988. Evidence for two calcium currents in insulin-secreting cells. *Pfluegers Arch. Eur. J. Physiol.* 411:401–409.